

**Support information of**  
**CFD simulation and high-speed photography of liquid flow**  
**in the outer cavity zone of a rotating packed bed reactor**

Yi Liu <sup>†,‡</sup>, Wei Wu <sup>†,‡</sup>, Yong Luo <sup>†,‡,\*</sup>, Guang-Wen Chu <sup>†,‡,\*</sup>,

Wei Liu <sup>†,‡</sup>, Bao-Chang Sun <sup>†,‡</sup>, Jian-Feng Chen <sup>†,‡</sup>

*<sup>†</sup> State Key Laboratory of Organic-Inorganic Composites and <sup>‡</sup> Research Center of the  
Ministry of Education for High Gravity Engineering and Technology, Beijing  
University of Chemical Technology, Beijing 100029, PR China*

\* Corresponding author: Tel: +86 10 64446466; Fax: +86 10 64434784.

E-mail address: luoyong@mail.buct.edu.cn; chugw@mail.buct.edu.cn

## **CT reconstruction**

The inner and outer diameters of rotor were 35 mm and 80 mm, respectively (Figure S1). Figure S2 indicates the step of CT reconstruction. If the threshold level was lower than the correct level, the packing structure reconstructed contained noisy points (Figure S2(a2)). If the threshold level was higher than the correct level, part of packing structure would be missing (Figure S2(c2)). Thus, a test for finding correct threshold level was instructed. The original 256-level greyscale images were divided into three parts: inner cavity, outer cavity, and packing zones. The inner and outer cavity zones didn't contain any information of packing structure and the packing zone was mainly considered. Several different threshold levels were tested from 0 ~ 50 level. At threshold of 35 level, the noisy points of inner and outer cavity zones were all eliminated (Figure S2(b2)) and then threshold of 35 level was selected for the reconstruction.

## **Droplet identification**

Figures S4 and S5 show the process to identify droplets. The boundaries of droplets in the photos were darker than the background. Like the photo below (Figure S4), the grayscale of background is about 204~211, while the grayscale of boundary for liquid droplet is about 126~136. Base on the difference grayscales, the droplet can be selected from the background with the help of Photoshop Quick Selection Tool. At least 9 pixels, a droplet could be identified from the photos.

## **Mathematical model**

### **VOF model**

The VOF model, generally used to compute a time-dependent solution, is based on

the description of the volumetric fraction of each phase in mesh cell. It relies on the fact that two or more phases are not interpenetrating. The mass conservation equation for the volume fraction function in the computational domain can be expressed as:

$$\frac{\partial(\alpha_q \rho_q)}{\partial t} + \nabla \cdot (\alpha_q \rho_q \vec{v}_q) = 0 \quad \text{with } q = g \text{ or } l \quad (1)$$

where subscripts  $l$  and  $g$  represent the liquid and gas phases, respectively;  $t$  is time, and  $\alpha_q$  is the volume fraction for phase  $q$ . The corresponding momentum balance equation for the two-phase flow is displayed as:

$$\frac{\partial(\rho \vec{v})}{\partial t} + \nabla \cdot (\rho \vec{v} \vec{v}) = -\nabla p + \nabla \cdot \left[ \mu \left( \nabla \vec{v} + \vec{v}^T \right) \right] + F_v \quad (2)$$

VOF model is a single set of conservation and momentum equations throughout the domain, and the resulting velocity field is shared among the phases. The mixture fluid properties, such as density  $\rho$  and dynamic viscosity  $\mu$ , are shared by the volume fraction of the different phases. The volume-averaged values are expressed as:

$$\rho = \sum \alpha_q \rho_q \quad (3)$$

$$\mu = \sum \alpha_q \mu_q \quad (4)$$

Besides, the volume fraction of each fluid in each computational cell is tracked throughout the domain. It can be computed based on the following constraint:

$$\sum_{q=1}^n \alpha_q = 1 \quad (5)$$

When the computational cell is full of  $q^{th}$  fluid,  $\alpha_q$  equals to one; in reverse,  $\alpha_q$  equals to zero. The interface between  $q^{th}$  fluid and one or more other fluids can be found in the cells with  $0 < \alpha_q < 1$ . In VOF model, the treatment of liquid interface is accomplished through the geometric-reconstruction scheme based on the piece linear

interface calculation (PLIC) method. The model stability is improved by the implicit body force formulation.

As a surface force, the surface tension can be converted into the volume force  $F_v$  by the continuum surface force (CSF) model.

$$F_v = \gamma \frac{\rho \kappa \hat{n}}{\frac{1}{2}(\rho_l + \rho_g)} \quad (6)$$

where  $\gamma$  is the surface tension coefficient and  $\kappa$  is the curvature of the interface defined as:

$$\kappa = \nabla \cdot \hat{n} \quad (7)$$

where  $\hat{n}$  is the surface normal ( $\hat{n} = n / |n|$ ) and  $n = \nabla \cdot \alpha_q$ .

### LES model

In LES model, an LES filter can be applied to a spatial and temporal field  $\varphi(x, t)$  and performs a spatial filtering operation, a temporal filtering operation, or both. The filtered field, denoted with a bar, is defined as:

$$\overline{\varphi(x, t)} = \int_{-\infty}^{\infty} \int_{-\infty}^{\infty} \varphi(r, t') G(x - r, t - t') dt' dr \quad (8)$$

where  $G$  is a filter convolution kernel.

For incompressible flow, the continuity equation and Navier–Stokes equation are filtered, yielding the filtered incompressible continuity Eq. (9) and the filtered Navier–Stokes Eq. (10).

$$\frac{\partial \bar{u}_i}{\partial x_i} = 0 \quad (9)$$

$$\frac{\partial \bar{u}_i}{\partial t} + \frac{\partial}{\partial x_j} (\overline{u_i u_j}) = -\frac{1}{\rho} \frac{\partial \bar{p}}{\partial x_i} + \nu \frac{\partial}{\partial x_j} \left( \frac{\partial \bar{u}_i}{\partial x_j} + \frac{\partial \bar{u}_j}{\partial x_i} \right) = -\frac{1}{\rho} \frac{\partial \bar{p}}{\partial x_i} + 2\nu \frac{\partial}{\partial x_j} S_{ij} \quad (10)$$

where  $\bar{p}$  is the filtered pressure field and  $S_{ij}$  is the rate-of-strain tensor.

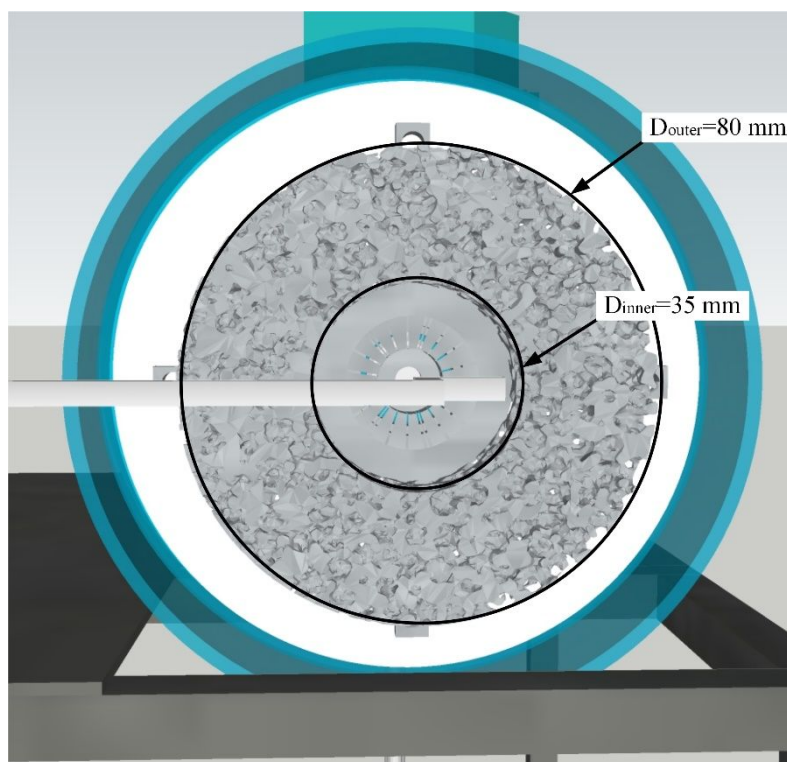


**Figure S1.** Size of rotor of RPB with nickel foam packing

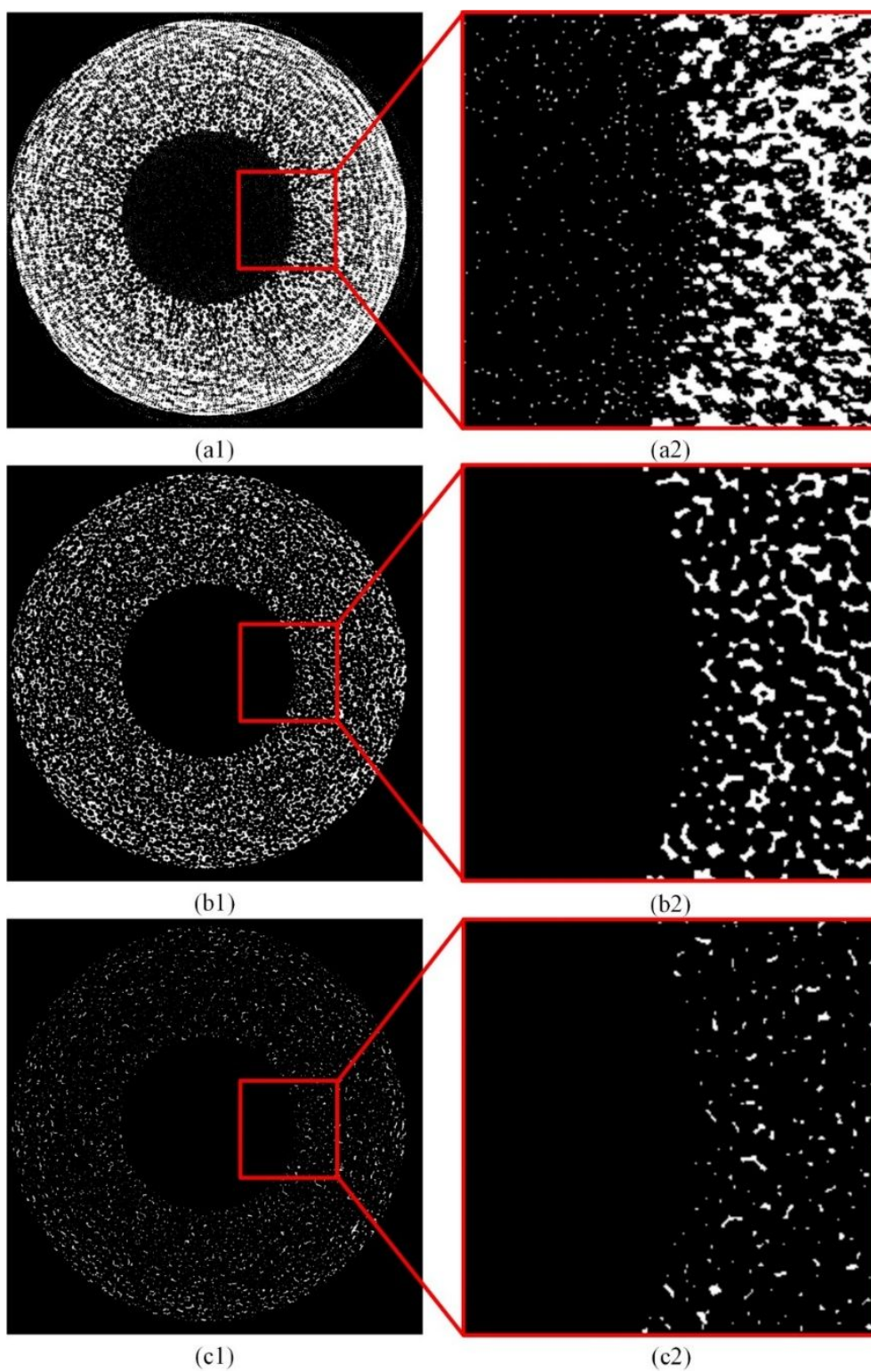


**Figure S2.** Binarized images of threshold of (a) 25, (b) 35, and (c) 45 levels (white part represent packing).

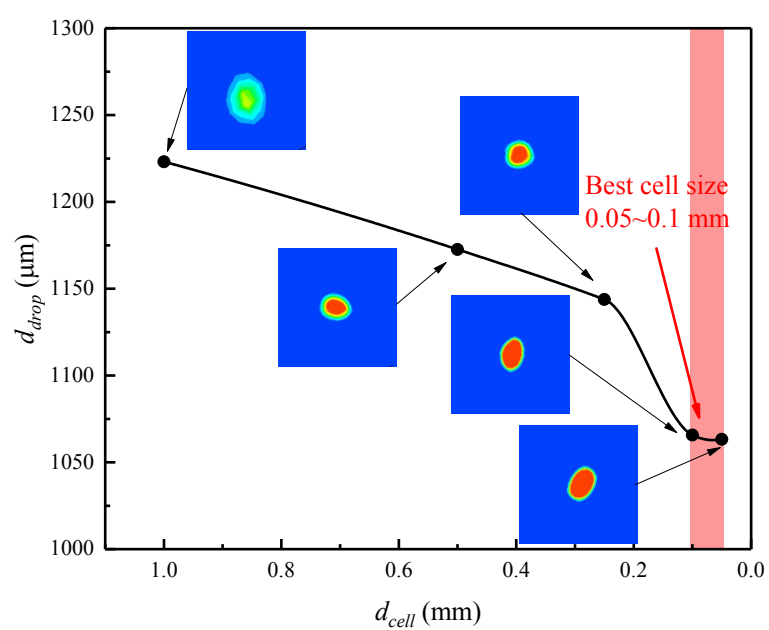


**Figure S3.** Effect of size of cell on liquid droplet diameter.

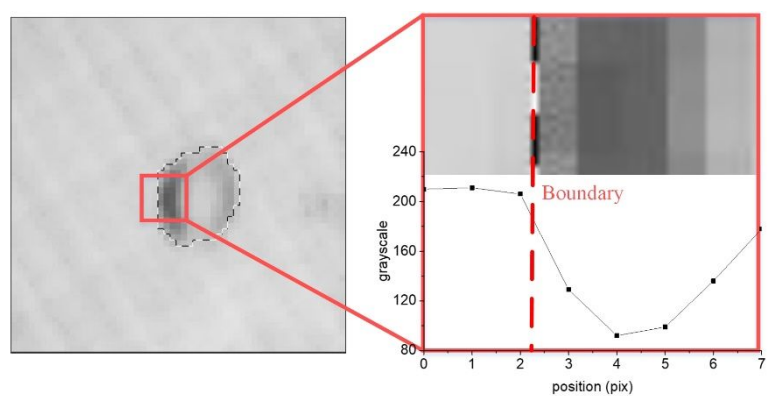


**Figure S4.** Identification of liquid droplet boundary.



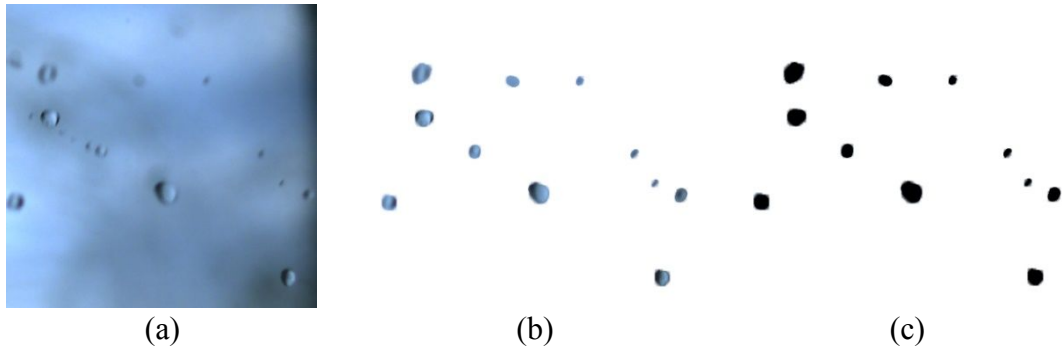


**Figure S5.** Process to identify droplets: (a) original photo; (b) segmented picture of droplets; (c) binary image.

**Table S1.** Computed liquid flow rates

$N$ (r/min)	$v_L$ (m/s)	Liquid flow rate (kg/s)		
		Nozzle tip	Inner peripherie of the outer cavity	Outlet (leaving the casing)
500	1.91	1.53	1.09	0.78
1000	1.91	1.53	0.66	0.32
1500	1.91	1.53	1.31	0.85
500	3.58	2.86	3.02	1.26
1000	3.58	2.86	2.67	2.62
1500	3.58	2.86	1.10	0.44